Supporting Information

Hierarchical architectures of mesoporous Pd on highly ordered TiO_2 nanotube arrays for electrochemical CO_2 reduction

Jinshuo Zou,[a] Muhammad Iqbal,[b,c] Amruthalakshmi Vijayakumar,[a] Caiyun Wang,[a] Douglas R. Macfarlane,[d] Yusuke Yamauchi,[b,c] Chong-Yong Lee,*[a] Gordon G. Wallace*[a]

[a] ARC Centre of Excellence for Electromaterials Science, Intelligent Polymer Research Institute, AIIM, Innovation Campus, University of Wollongong, Wollongong, NSW 2500, Australia

[b] Key Laboratory of Eco-chemical Engineering, College of Chemistry and Molecular Engineering, Qingdao University of Science and Technology (QUST), Qingdao 266042, P. R. China

[c] School of Chemical Engineering, Faculty of Engineering, Architecture and Information Technology (EAIT), University of Queensland, Brisbane, QLD 4072, Australia

[d] School of Chemistry, Monash University, Clayton, VIC 3800, Australia

Corresponding Author

* Chong-Yong Lee. E-mail: cylee@uow.edu.au.

* Gordon G. Wallace. E-mail: gwallace@uow.edu.au.

Table S1. Summary of reported Pd-based catalysts for CO_2 electroreduction with formate as a targeted product

Sample	Structure	Electrolyte	Potential (V vs. RHE)	Faradaic efficiency (%)	Reference
Pd nanoparticles	~5 nm Pd nanoparticles on carbon particles	2.8 M $KHCO_3$	-0.05 V ~ -0.25 V	Formate: 86 to 94 %	Min and Kanan [1]
Pd nanoparticles	3.7 nm nanoparticles	1 M $KHCO_3$	-0.1 V ~ -0.2 V	Formate: ~98 %	Gao et al. [2]
Boron-doped Pd	4.1± 0.5 nm	0.1 M $KHCO_3$	-0.5 V	Formate: 70%	Jiang et al. [3]
Pd nanoparticles	~ 4.2 nm Pd nanoparticles	0.5 M $NaHCO_3$	-0.15 V	Formate: 71%	Takashima et al. [4]
Pd@TiO_2/ Carbon Nanohorns	Pd nanoparticles (1.5 nm) shielded within the TiO_2 phase	0.5 M $NaClO_4$	~ -0.2 V vs. RHE	Formate: ~95% in the initial 5 min, 40% after 1 h	Melchionna et al. [5]
RuO_2 + TiO_2	RuO_2:TiO_2=35:65 (mole percent)	0.05M H_2SO_4 (pH = 12)	-0.9 V vs. Hg_2SO_4	Formate: ~2%	Bandi et al. [6]
RuO_2 + MoO_2 + TiO_2	RuO_2:MoO_2:TiO_2= 25:30:45 (mole percent)	0.05M H_2SO_4 (pH = 12)	-0.9 V vs. Hg_2SO_4	Formate: <1%	Bandi et al. [6]
RuO_2 + Co_3O_4 + SnO_2 + TiO_2	RuO_2:Co_3O_4:SnO_2: TiO_2= 20:10:8:62 (mole percent)	0.05M H_2SO_4 (pH = 12)	-0.9 V vs. Hg_2SO_4	Formate: 18%	Bandi et al. [6]
mPd/TNTAs	MesoporousPd-TiO_2 nanotube hierarchical structures	0.5 M $NaHCO_3$	-0.1 V	Formate: 88%	This work

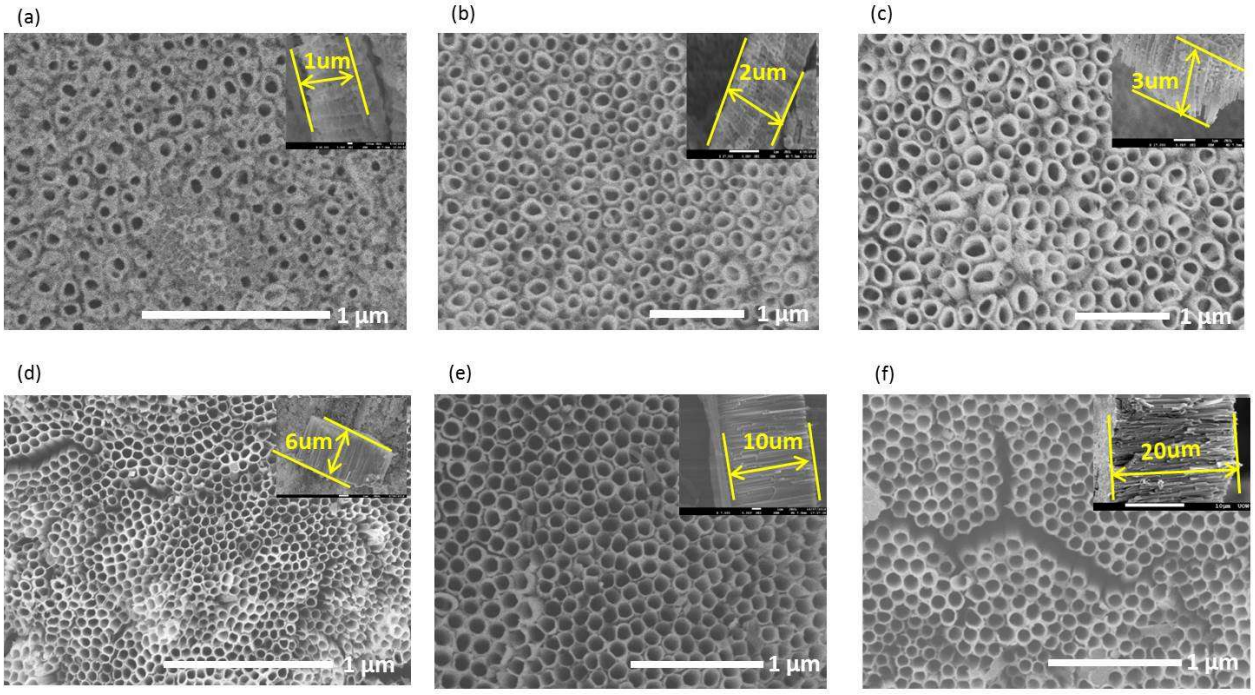

Fig. S1 SEM images of TiO_2 nanotube arrays of different tube lengths: (a) 1 µm, (b) 2 µm, (c) 3 µm, (d) 6 µm, (e) 10 µm, (f) 20 µm.

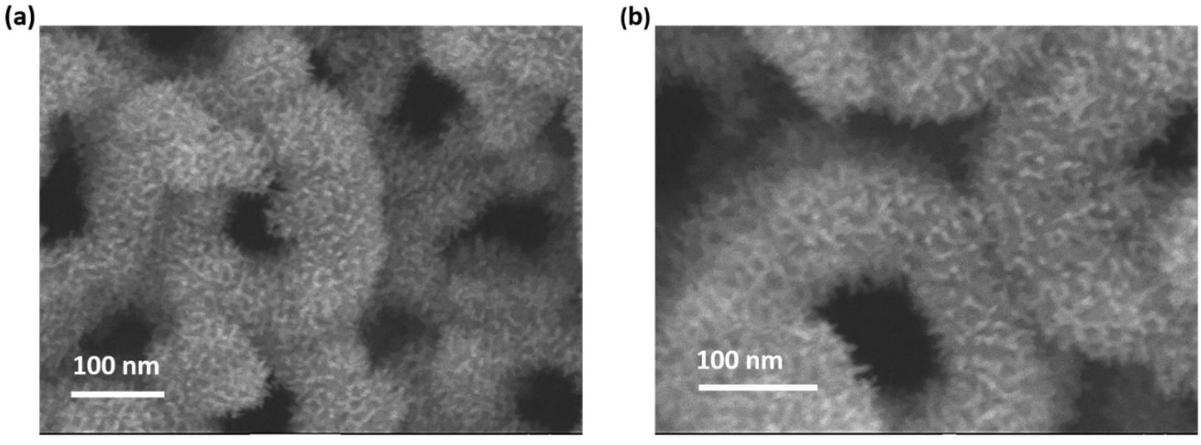

Fig. S2 SEM images of mPd/TNTAs with higher resolution.

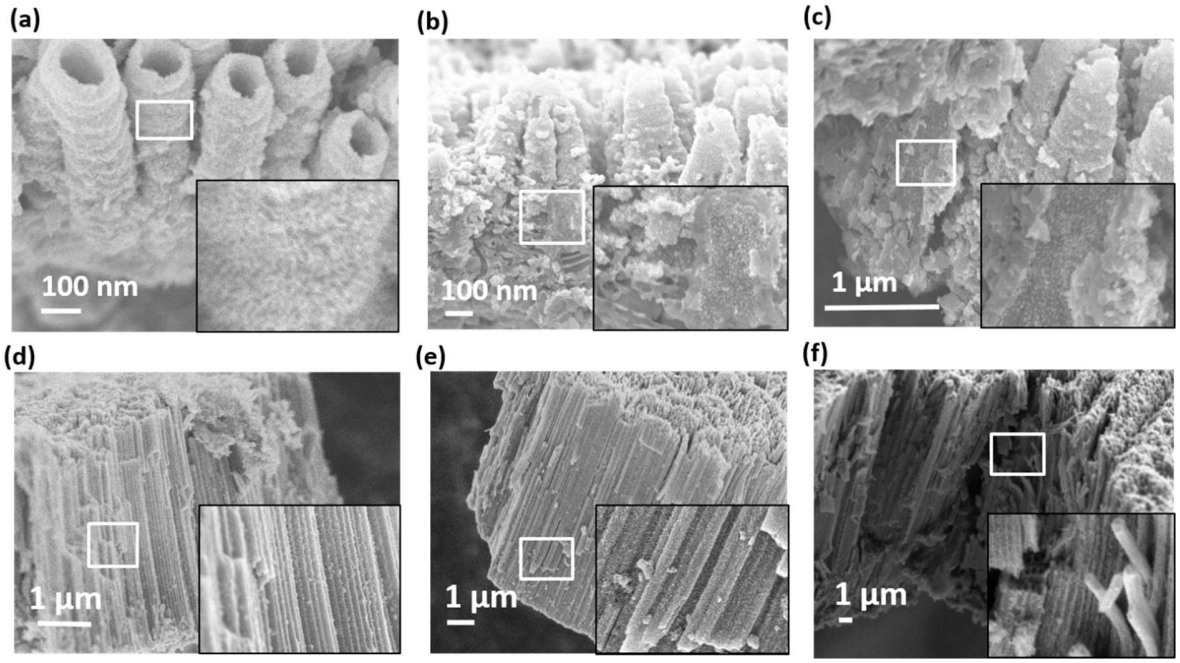

Fig. S3 SEM images of mPd/TNTAs with different tube lengths: (a) 1µm, (b) 2 µm, (c) 3 µm, (d) 6 µm, (e) 10 µm, (f) 20 µm.

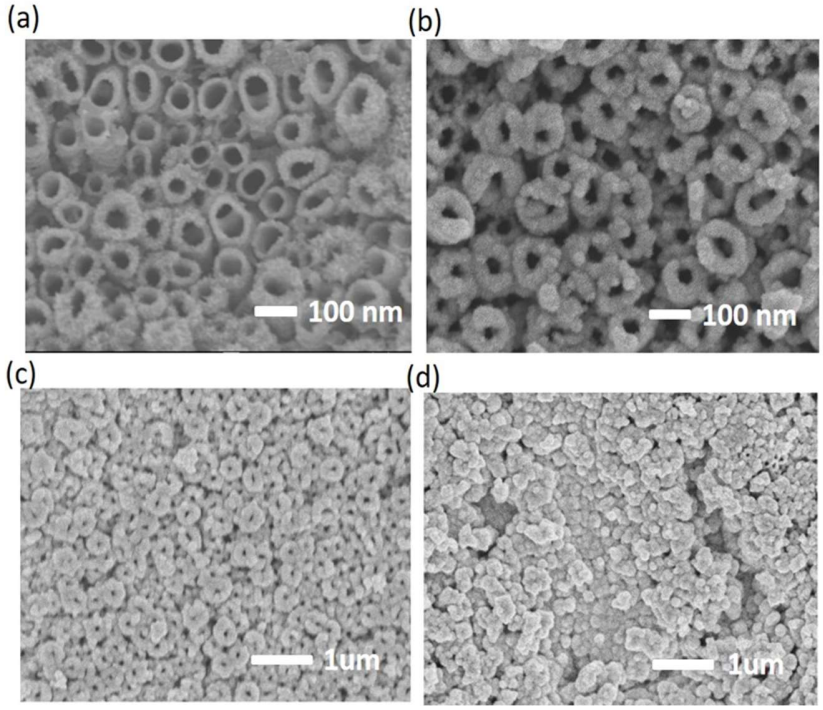

Fig. S4 SEM images of mPd/TNTA samples with different electrodeposition time: (a) 1 min, (b) 2 min, (c) 3 min, (d) 5min

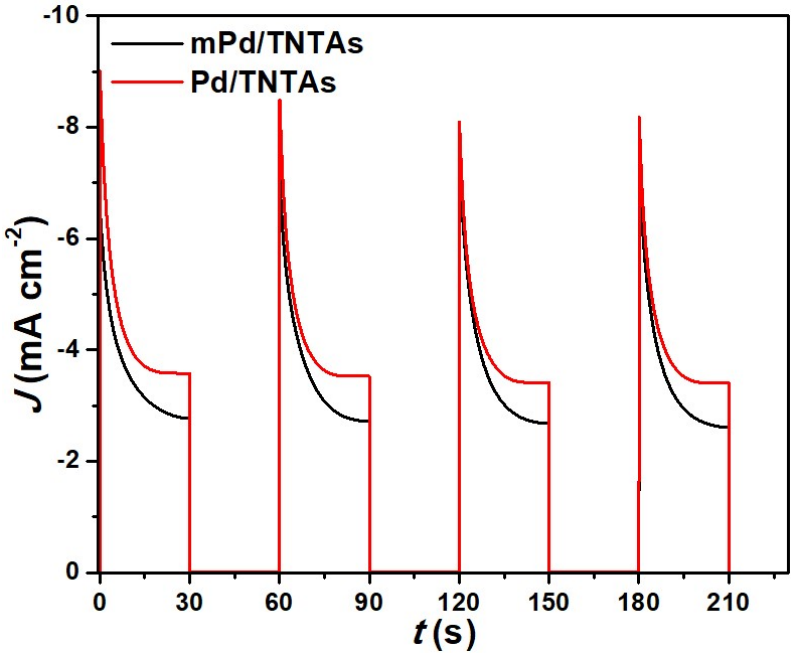

Fig. S5 Current-time curves of mPd/TNTAs and Pd/TNTAs during the electrodeposition.

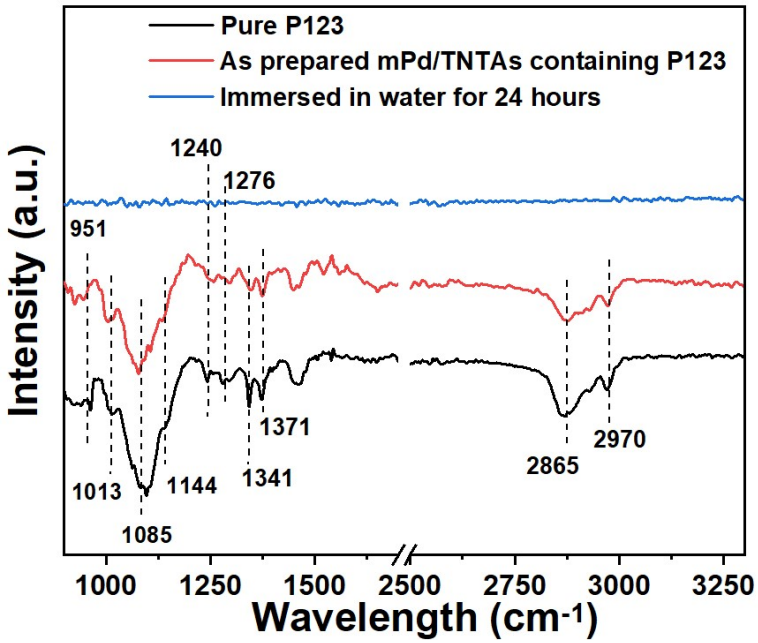

Figure S6. FTIR of pure P123, as prepared mPd/TNTAs containing P123 micelles, and after immersing in water for 24 h.

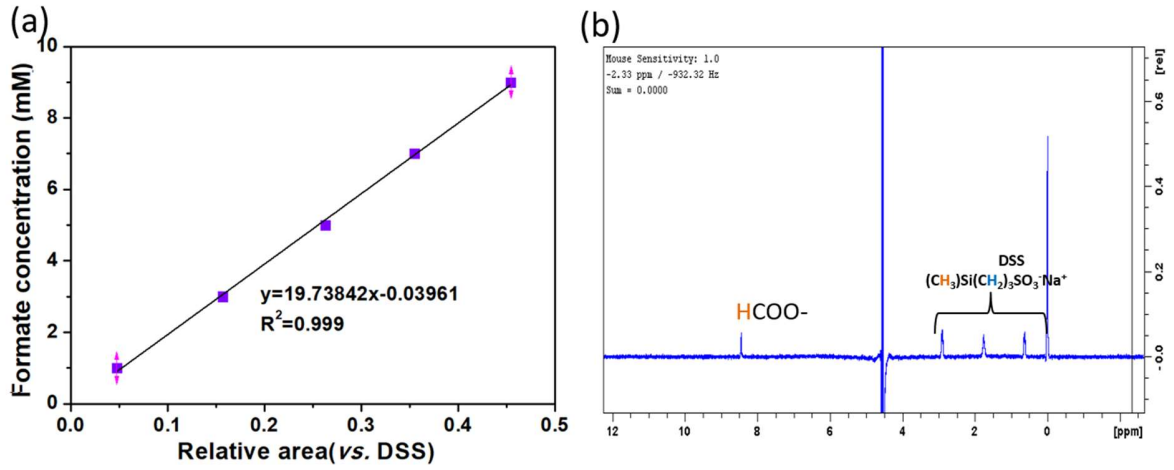

Fig. S7 (a) the linear relationship between the formate concentration and the relative area (vs. DSS); (b) the 1H-NMR spectrum for formate. The single peak at 8.44 ppm coresponding to the H in formate and the peak at 0.00 ppm represents the internal standard DSS. The relative areas were calculated based on the equation:

$$Relative\ area(Formate) = Peak\ area\ at\ 8.44\ ppm / Peak\ area\ at\ 0.00\ ppm$$

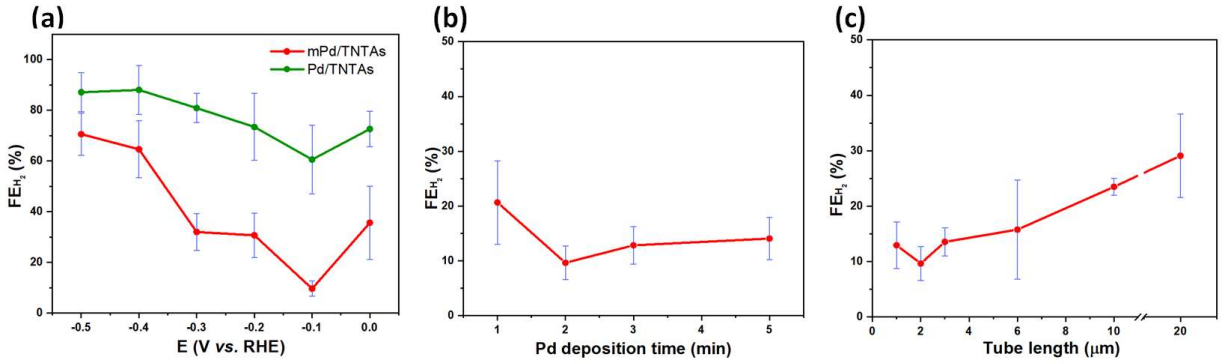

Fig. S8 Comparison of H_2 faradaic conversion efficiencies of mPd/TNTAs and Pd/TNTAs as a function of applied potential (a), H_2 faradaic conversion efficiencies of mPd/TNTAs with different mPd loading time (b) and different length of the TiO_2 nanotube arrays of mPd/TNTAs (c). (a, b) based on TNTAs of 2 μm; (a, c) mPd loading time of 2 min, and (b, c) at -0.1 V vs. RHE. All experiments were performed in 0.5 M $NaHCO_3$ aqueous solution under constant purging of CO_2 (20 mL min^{-1}) for 1 h.

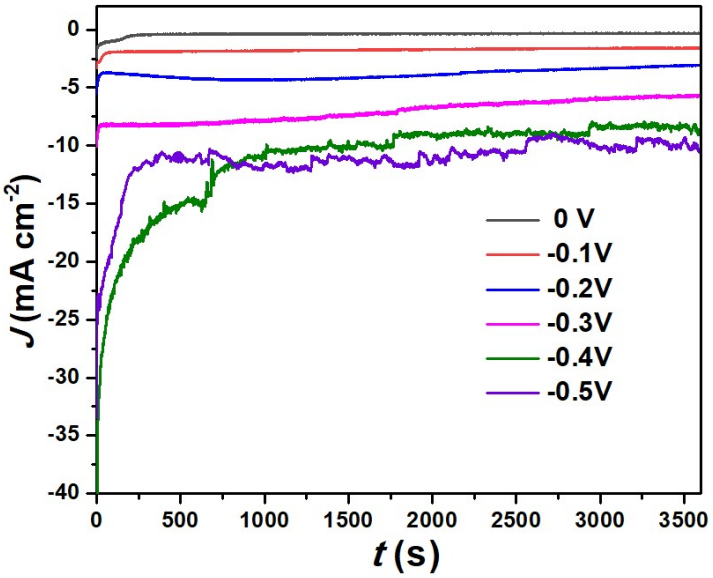

Fig. S9 Current density-time curves of mPd/TNTAs at the potential range of 0 to -0.5 V vs. RHE.

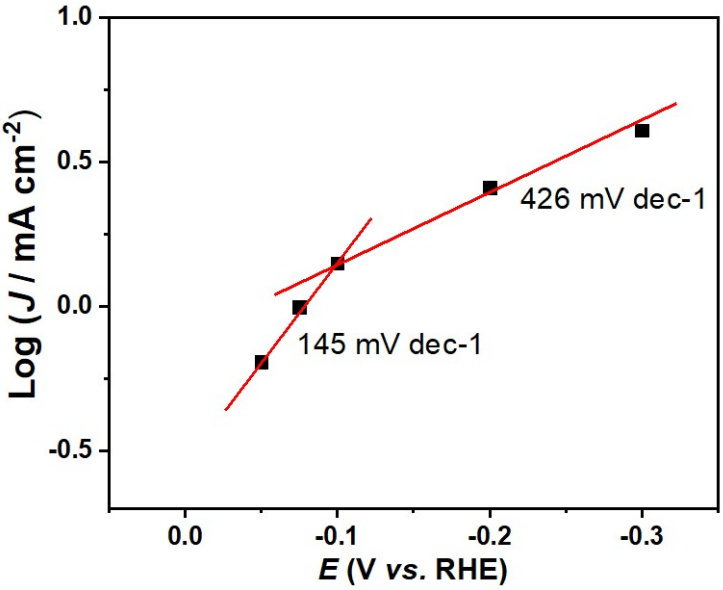

Fig. S10 Tafel plot of the mPd/TNTAs at the potentials between 0 to -0.3 V *vs.* RHE.

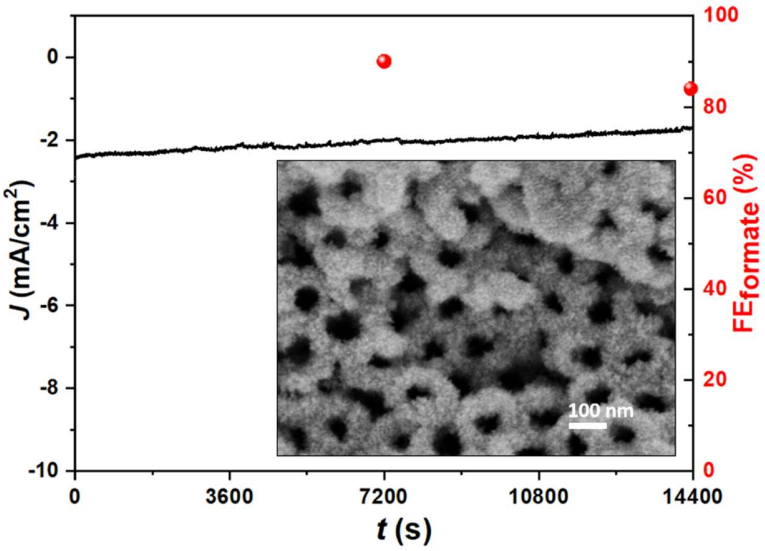

Fig. S11 The long term CO_2RR stability test of the mPd/TNTAs samples performed at - 0.10 V *vs.* RHE. Inset showing the SEM of mPd/TNTAs after the 4 h electrochemical CO_2RR.

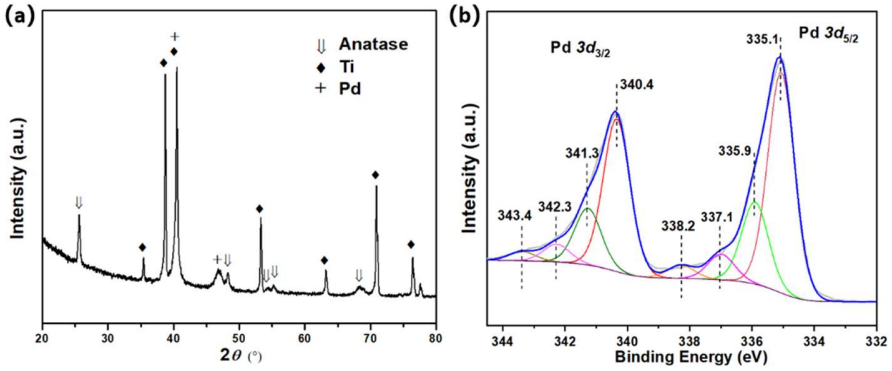

Fig. S12 (a) XRD pattern and (b) XPS spectrum of the mPd/TNTAs after CO_2 reduction performance test of 4 hours.

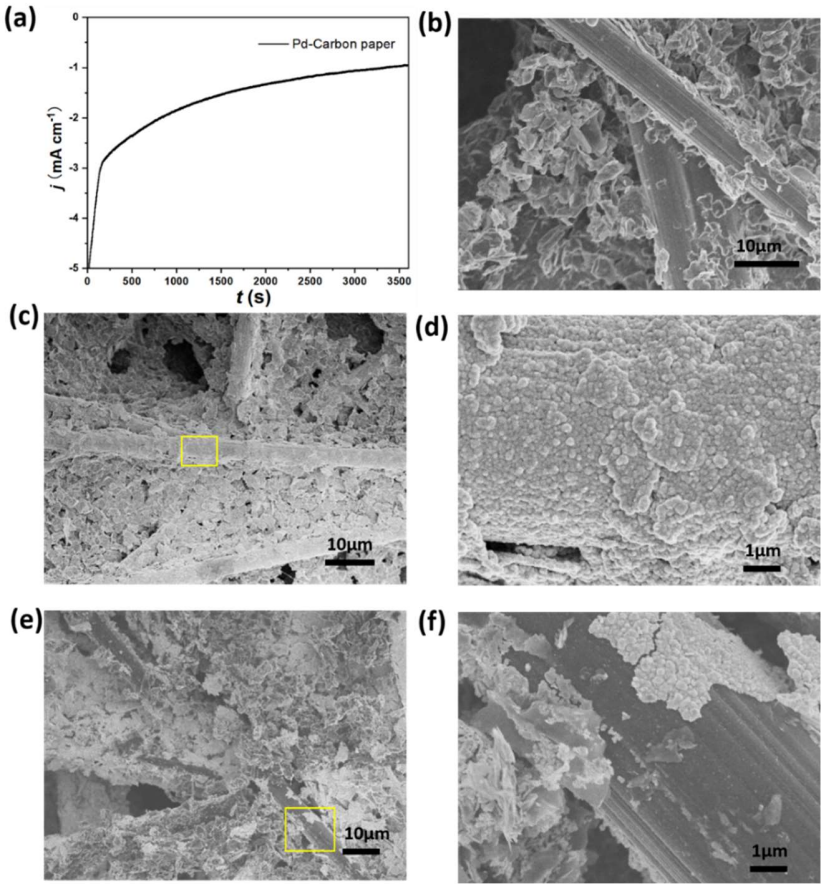

Fig. S13 (a) Current density vs. time of mesoporous Pd on carbon paper. SEM image of (b) carbon paper, (c-d) mesoporous Pd on carbon paper before test, and (e-f) after test. (d) and (f) are the enlarged areas in the selected areas in (c) and (e), respectively. The CO_2RR performace test were conducted in CO_2 saturated $NaHCO_3$ (0.5M) aqueous solution under constant purging of CO_2 (20 mL min^{-1}) for 1 h. The mesoporous Pd on carbon paper was electrodeposited for 2 min.

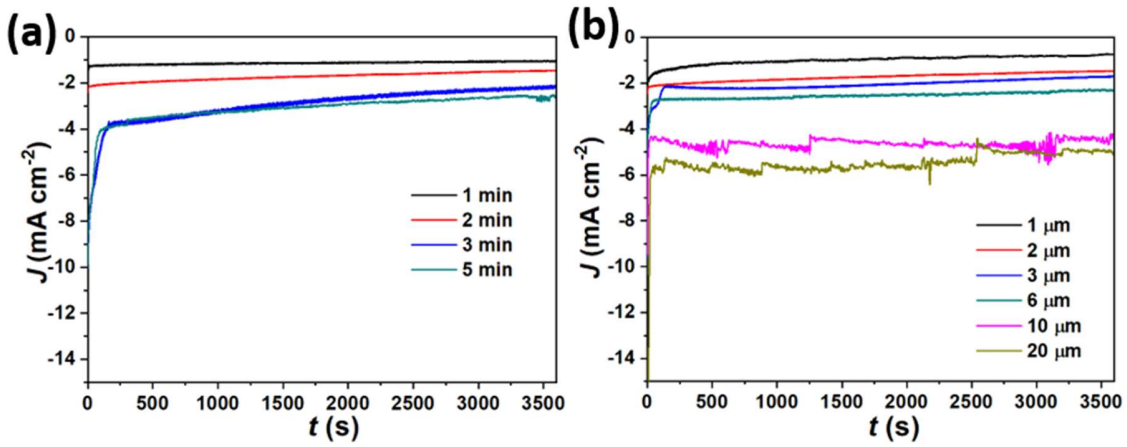

Fig. S14 Current density-time curves of mPd/TNTAs with (a) different Pd layer thicknesses and TiO_2 (b) nanotube lengths, with an applied potential of -0.10 V *vs.* RHE.

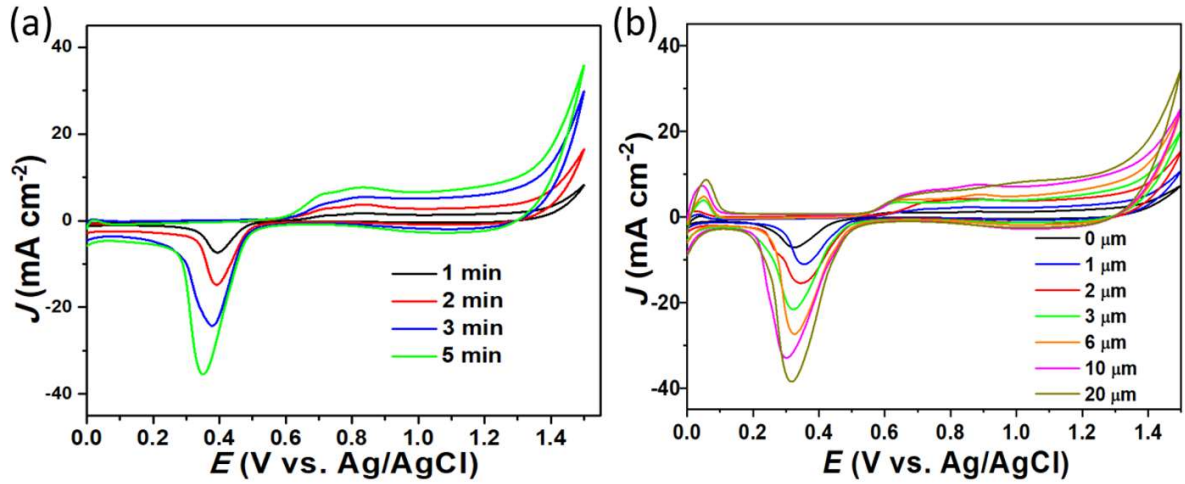

Fig. S15 CV measurements of (a) mPd-TNTAs (2 μm) with different Pd deposition time; (b) mPd-TNTAs with different TNTAs lengths, the loading time in (b) is 2 min. All the measurements were performed in 0.5 M H_2SO_4.

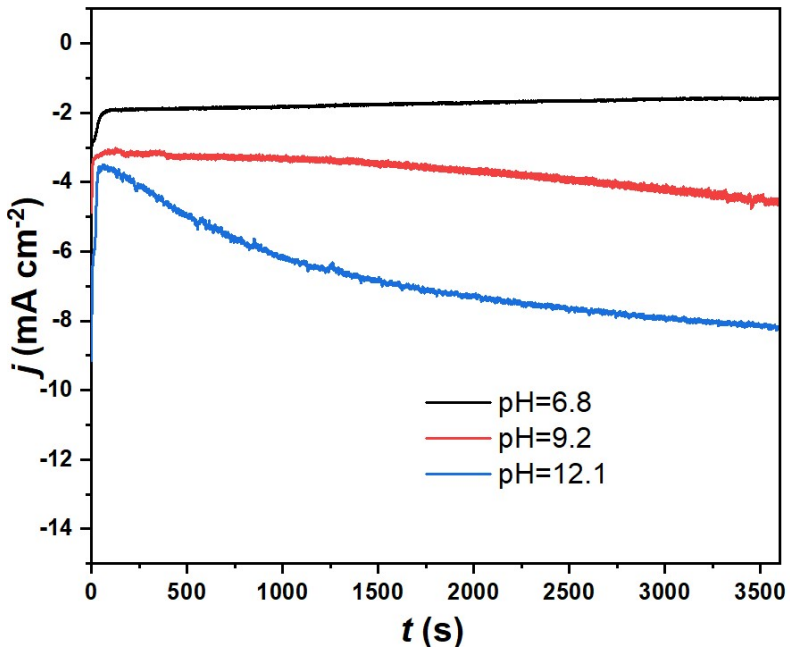

Fig. S16 Current density-time curves of mPd/TNTAs with different initial pH. All experiments were performed in 0.5 M $NaHCO_3$ aqueous solution under constant purging of CO_2 (20 mL min^{-1}) for 1 h using the mPd/TNTAs of 2min mesoporous Pd loading and TiO_2 tubes of 2 µm.

References

[1] X. Min, M. W. Kanan, *J. Am. Chem. Soc.* **2015**, *137*, 4701-4708.

[2] D. Gao, H. Zhou, F. Cai, D. Wang, Y. Hu, et al., *Nano Res.* **2017**, *10*, 2181-2191.

[3] B. Jiang, X.-G. Zhang, K. Jiang, D.-Y. Wu, W.-B. Cai, J. Am. Chem. Soc. 2018, 140, 2880-2889.

[4] T. Takashima, T. Suzuki, H. Irie, *Electrochemistry* **2019**, *87*, 134-138.

[5] M. Melchionna, M. V. Bracamonte, A. Giuliani, L. Nasi, T. Montini, et al., *Energ. Environ. Sci.*, **2018**, *11*, 1571-1580.

[6] A. Bandi, *J. Electrochem. Soc.*, **1990**, *137*, 2157.